applied sciences

MDPI

Article

A Method for Synthesizing Iron Silicate Slags to Evaluate Their Performance as Supplementary Cementitious Materials

Anton Andersson [1,*], Linus Brander [2], Andreas Lennartsson [1], Åke Roos [3] and Fredrik Engström [1]

[1] Division of Minerals and Metallurgical Engineering, Luleå University of Technology, SE-971 87 Luleå, Sweden; andreas.lennartsson@ltu.se (A.L.); fredrik.i.engstrom@ltu.se (F.E.)
[2] Division of Built Environment—Infrastructure and Concrete, Research Institute of Sweden, SE-501 15 Borås, Sweden; linus.brander@ri.se
[3] Boliden AB, SE-101 20 Stockholm, Sweden; ake.roos@boliden.com
* Correspondence: anton.andersson@ltu.se

Abstract: Utilizing iron silicate copper slag as supplementary cementitious material (SCM) is a means to improve resource efficiency and lower the carbon dioxide emissions from cement production. Despite multiple studies on the performance of these slags in SCM applications, the variations in cooling procedure, grinding, and methods for evaluating reactivity limit the ability to assess the influence of chemical composition on reactivity from the literature data. In this study, a methodology was developed to synthesize iron silicate slags, which were then evaluated for their inherent reactivity using the R^3 calorimeter-based experiments. The results demonstrated that laboratory-scale granulation produced the same reactivity as industrially granulated slag. Furthermore, a synthesized triplicate sample showed high repeatability. Based on these two aspects, this method can be used to systematically study the influence of chemical composition on the inherent reactivity of iron silicate slags while producing results that are directly translatable to industrial slags.

Keywords: synthetic iron silicate glass; copper slag; supplementary cementitious material; recycling; circularity

Citation: Andersson, A.; Brander, L.; Lennartsson, A.; Roos, Å.; Engström, F. A Method for Synthesizing Iron Silicate Slags to Evaluate Their Performance as Supplementary Cementitious Materials. *Appl. Sci.* **2023**, *13*, 8357. https://doi.org/10.3390/app13148357

Academic Editor: Bing Chen

Received: 22 June 2023
Revised: 10 July 2023
Accepted: 17 July 2023
Published: 19 July 2023

1. Introduction

Copper production is associated with high slag rates; on average, 2.2–3.0 tons of slag are generated per ton of produced copper [1,2]. Based on these figures combined with data on copper production [3], the worldwide annual generation of copper slag is between 47 and 64 million tons. Undoubtedly, the slag must be utilized to ensure sustainable copper production from a resource-efficiency standpoint.

Several external applications for copper slag have been reported, e.g., various construction applications excluding cement and concrete [1,2,4,5], blasting abrasive media [2,4–6], auxiliary sand in concrete [1,2], and for its pozzolanic properties, i.e., as supplementary cementitious material (SCM) [1,2]. Since the cement industry accounts for 5–8% of global anthropogenic carbon dioxide emissions [7,8], utilizing copper slag in cementitious applications is an attractive alternative. Using the slag as an SCM would improve resource efficiency while lowering carbon dioxide emissions per ton of cementitious material. The former effect is obvious, i.e., the lower requirements for the generation of virgin material, while the latter relates to the fact that the SCM requires neither calcination nor clinkering [9].

A study on the possibility of using copper slag as an SCM was performed by Tixier et al. [10] in 1997. The results showed that the incorporation of the slag improved the compressive strength of mortars after curing beyond seven days [10]. Since 1997, several studies have been published explicitly addressing iron silicate copper slags for SCM applications [6,11–20]. Furthermore, an additional study has incorporated the slag in a comparison of different

SCMs [21]. The slag compositions included in these studies are presented in Table 1. The primary methodologies employed for these slags include mortar testing [6,11–14,16,18,21], cement composite testing [17,19,20], isothermal calorimetry on Portland cement blends [12,14,19,20], isothermal calorimetry using the R^3 test [21], as well as the Chapelle and Frattini tests [14].

Table 1. Summary of slag compositions evaluated for SCM purposes in the literature. The reported concentrations [wt%] were rounded to one decimal point. The FeO/SiO_2 ratio was, however, calculated based on the reported values from the authors.

Ref.	FeO/SiO_2	FeO [1]	SiO_2	CaO	Al_2O_3	MgO	ZnO [1]	Cu [1]
[17]	1.12	37.9	33.9	12.7	4.7	0.8	/	/
[19]	1.14	37.9	33.3	12.3	4.6	1.1	1.3	1.4
[19]	1.14	36.9	32.3	19.5	3.9	0.9	1.2	1.2
[16,21]	1.14	36.8	32.3	3.9	11.0	/	/	/
[19,20]	1.27	42.3	33.4	4.0	3.5	1.4	1.1	/
[10]	1.35	47.5	35.2	3.3	5.0	0.6	/	0.5
[6]	1.46	48.1	33.1	6.1	2.8	1.6	/	0.4
[15]	1.49	46.9	31.5	3.2	8.5	4.4	0.3	1.3
[14]	1.58	40.9	25.9	7.1	5.9	0.8	8.8	0.3
[12]	1.80	54.0	30.1	0.6	4.0	0.8	/	/
[13]	1.98	55.5	28.0	2.5	4.0	1.2	/	0.7
[11]	2.15	56.0	26.0	2.0	3.3	2.7	0.9	1.1

[1] Analyses given for different oxidation states (0, +I, +II, or +III) were recalculated to FeO, ZnO, and Cu to enable the comparison.

The studies have concluded that iron silicate copper slags exhibit pozzolanic properties [12,14–16,21]. However, the inherent reactivity is lower than, e.g., ground granulated blast furnace slag [21,22], which is reflected when reviewing data on mortars and cement composites. More specifically, the data presented after the study by Tixier et al. [10] is ambiguous in terms of the contribution to the strength development. Several studies have shown that partial replacement of Portland cement with copper slag improves strength [11,13], whereas other studies have shown negative effects [6,12,14,16]. Nonetheless, accounting for the replacement ratio used in the different studies, the overall conclusion is that iron silicate copper slags contribute to the strength of both mortars [11–14,16] and composites [17,19].

The reactivity of SCMs depends on such parameters as the degree of crystallinity, glass structure, thermal history, granulometric properties, and chemical composition [23–30], which, naturally, have not been constant between the different studies discussed in relation to Table 1. In addition, the summary of the methodologies utilized in the different studies highlights the fact that different means to assess the reactivity of the copper slags have been employed. Therefore, the previously published data cannot be used across different papers to offer insight into how variations in chemical composition affect the reactivity of copper slags. However, two studies have subjected slags of different compositions to testing at the same laboratory [18,19]. The study by Wang et al. [18], comparing ten different copper slags, did not focus on the compositional aspect, which provides challenges in assessing their data in this manner. On the other hand, Feng et al. [19] conducted laboratory-scale experiments to change the calcium oxide content of an industrial slag systematically. The results showed that the strength of cement composites improved with higher calcium oxide contents, which is consistent with results on the dissolution kinetics of other SCMs [27].

Considering the compositions presented in Table 1, variations beyond the calcium oxide content are apparent when comparing slags from different smelters. Therefore, the effect of changes in concentrations of other constituents than calcium oxide on the reactivity is of interest. The literature data on other systems can be used to indicate the effect of other constituents. Studies have shown that the degree of polymerization affects the dissolution behavior of SCMs [27,28]. In iron silicate copper slags, the FeO/SiO_2 ratio plays a significant role in deciding the polymerization of the silicate network. Thus, since the

role of iron in supplementary cementitious reactions is not fully understood [31,32], the effect of polymerization in iron silicate slags is, most likely, not straightforward. Furthermore, the effect of alumina content has been presented for other systems [9,27], but, as apparent from Table 1, the range of the alumina content, and differences in concentrations of cations available for charge-balancing aluminum in the silicate network, indicate an intricate relationship.

In conclusion, the literature suggests that iron silicate copper slags are suitable to incorporate in SCM applications. However, data on how components beyond calcium oxide affect the performance of the iron silicate slag as an SCM is lacking. This observation highlights the need for controlled studies on the effect of changes in chemical composition on the reactivity of iron silicate slags. Feng et al. [19] used an industrial slag as the base material for changing the chemical composition. Ideally, synthetic slags generated in laboratory scale experiments should be aimed at since this approach would allow the composition to be extended beyond the operational window of a specific smelter. Studies on synthesizing iron silicate copper slags on a laboratory scale for subsequent evaluation of performance as SCM could not be found in the literature. Therefore, the present paper aims to develop a method for synthesizing iron silicate slags, which can be employed to produce relevant and repeatable data and, consequently, open the field to study the effect of chemical composition on reactivity.

2. Theoretical Considerations

To address the aim, the means required to synthesize the iron silicate slag system were reviewed. Three challenges were as follows: (i) controlling the partial pressure of oxygen to avoid oxidation of ferrous iron; (ii) choosing a crucible system that allows for controlled variations of the slag's components; and (iii) choosing a crucible system that allows simple handling of water granulation in laboratory scale experiments.

Concerning the first point, zinc fuming processes designed to remove zinc from iron silicate copper slags drive the reduction close to the precipitation of iron if the process aims for maximum zinc removal [33]. This information offers a basis for the partial pressure of oxygen required to synthesize a slag with the correct oxidation state of iron. Pyrometallurgical experiments with controlled oxygen partial pressures are commonly performed in gas-tight tube furnaces where calculated mixtures of carbon monoxide and carbon dioxide at fixed temperatures are used [34,35]. Although this approach is suitable in other experimental designs, the setup offers challenges when water granulation of the synthesized slag is desired. Most importantly, breaking the atmosphere would cause poisonous carbon monoxide to exit the gas-tight equipment and spread to the vicinity of the furnace.

Another approach to control the partial pressure of oxygen is to use an iron crucible. According to Mysen and Richet [36], using an iron crucible will provide an oxygen buffer to the system. The benefit of this is evident when considering fumed slags that are driven close to the reduction of ferrous iron. Figure 1 illustrates the 1300 °C isothermal section (a reasonable experimental temperature in accordance with Section 3.2) of the FeO-Fe_2O_3-SiO_2 phase diagram. Assuming that the FeO/SiO_2 ratio is designed to avoid cristobalite and monoxide, the iron crucible will buffer the oxidation state of iron within the phase field of iron and slag. Naturally, an inert atmosphere in combination with the crucible must be employed to mitigate the excessive introduction of iron atoms into the slag system.

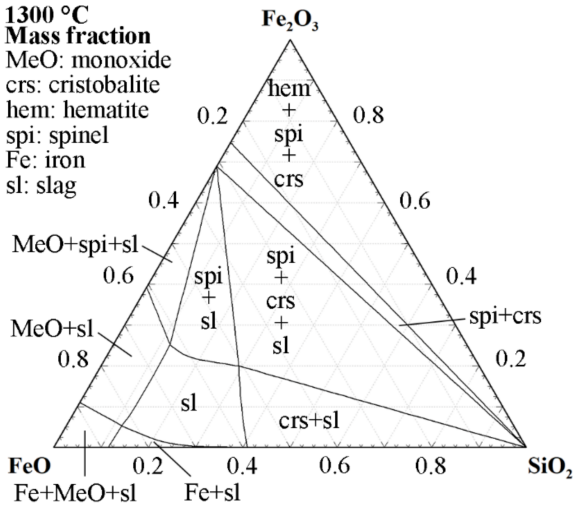

Figure 1. 1300 °C isothermal section of the FeO-Fe_2O_3-SiO_2 phase diagram with activity of Fe = 1. Calculated using the Phase Diagram module of FactSage 8.2 with the GTOx and FactPS databases [37–39].

Regarding the second challenge, i.e., finding a crucible system that minimizes the slag–crucible interactions and, thus, allows for controlled variations in the chemical composition, considerations of phase equilibria must be taken into account. No crucible–slag system is inert at high temperatures, which was highlighted by the careful selection of crucibles based on the origin of different steel slags in the study by Tossavainen et al. [40]. A common approach to avoid extensive slag–crucible reactions is to use platinum. This approach was adopted by Schöler et al. [27] and Snellings [28] in the syntheses of blast furnace slags and calcium aluminosilicate glasses, respectively. For iron silicate slags, using platinum is impossible due to the iron–platinum solubility and the formation of intermediate compounds [36].

Another method to minimize interactions with the crucible is to use a ceramic system and saturate the slag with the component representing the crucible. This method was used for basic oxygen furnace (BOF) slags saturated in magnesia by Lee and Fruehan [41]. In BOF steelmaking, this approach has industrial relevance since magnesia-saturated slags minimize refractory wear [41]. For iron silicate slags, the solubility of fayalite and forsterite, in combination with the progressively higher melting points of olivine toward higher magnesium contents [42], makes magnesia crucibles unsuitable. Although industrial slags are more complex, the phase diagram of the three-component system, including magnesia and the two major components of the slag, i.e., FeO-SiO_2, can be used to demonstrate the slag crucible interaction. Figure 2 illustrates the isothermal section at 1300 °C of the FeO-SiO_2-MgO system. The phase diagram shows that the slag phase is never in a two-phase equilibrium with magnesia. Assuming that the mass of the crucible exceeds that of the slag, equilibrating the phases means that the slag will form olivine and, subsequently, move into the phase field of olivine and monoxide, i.e., magnesiowüstite. On the other hand, if the slag phase exists in excess, the magnesia crucible could be consumed by the reaction with the slag.

The remelting and modification of iron silicate slags, performed by Feng et al. [19], was achieved using alumina crucibles. Figure 3 illustrates that alumina is readily soluble in iron silicate slags. However, as opposed to using magnesia crucibles, iron silicate slags can be saturated in alumina, as shown by the phase fields where both corundum and slag are present. Based on the results presented by Feng et al. [19], the remelting of the industrial slag did not cause severe changes in the alumina content, which highlights that kinetic limitations favor the use of this ceramic system. Nonetheless, synthesizing slags from chemical reagents using a crucible made of a component that, in fact, is a desired variable is not attractive when aiming to evaluate the effect of chemical composition. In

addition, Figure 3 suggests that different starting conditions regarding the FeO/SiO_2 ratios will translate to different possible alumina contents when moving toward equilibrium.

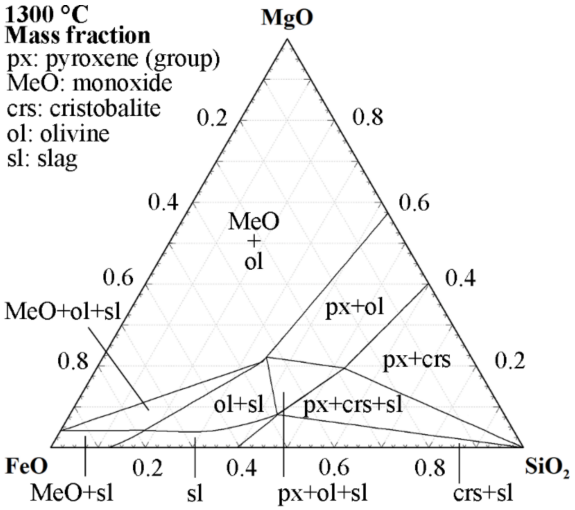

Figure 2. The 1300 °C isothermal section of the FeO-SiO_2-MgO phase diagram with activity of Fe = 1. Calculated using the Phase Diagram module of FactSage 8.2 with the FToxid and FactPS databases [39].

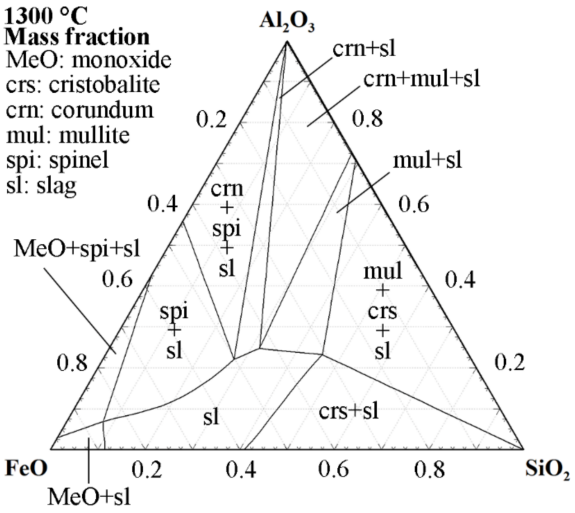

Figure 3. The 1300 °C isothermal section of the FeO-SiO_2-Al_2O_3 phase diagram with activity of Fe = 1. Calculated using the Phase Diagram module of FactSage 8.2 with the GTOx and FactPS databases [37–39].

Another ceramic system is zirconia, which has been used by Anindya et al. [43] for iron silicate slag. Based on the three-component diagram, Figure 4, the solubility of zirconia in the slag is significantly lower than alumina. Nonetheless, the application of this system was found to be inappropriate for the experiments performed by Anindya et al. [43], who reported catastrophic failure of the crucible. Based on the present authors' experience, yttria-stabilized zirconia functions well for industrial iron silicate slags in experiments where remelting is desired. However, to allow for simple handling and water granulation of the slag, ceramic crucibles, such as zirconia and alumina, are less attractive due to their brittleness at high temperatures.

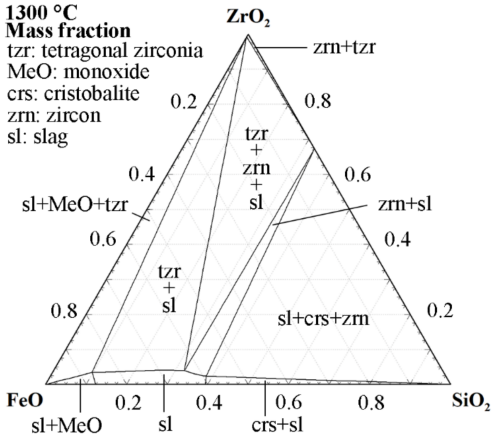

Figure 4. The 1300 °C isothermal section of the FeO-SiO_2-ZrO_2 phase diagram with activity of Fe = 1. Calculated using the Phase Diagram module of FactSage 8.2 with the FToxid and FactPS databases [39].

The challenge of granulating iron silicate slag from ceramic crucibles on a laboratory scale, i.e., the third challenge identified above, is exemplified by the experimental setup used by Feng et al. [19]. In that study, using alumina crucibles necessitated an experimental setup using a tiltable induction furnace and intricate design to maintain the crucible from falling during tapping [19]. The third challenge can be addressed using iron crucibles since they are not brittle nor subjected to thermal shock. Therefore, these crucibles can be handled manually at temperatures relevant to iron silicate slags.

Furthermore, the pure oxides of common components in iron silicate slags, e.g., calcium oxide, magnesia, and alumina, are more stable than ferrous oxide (Figure 5). Naturally, the partial pressure required for reducing the oxides in the solution is different. However, Figure 5 illustrates that iron is not a strong reducing agent in comparison to silicon, aluminum, magnesium, and calcium. In contrast, according to the figure, syntheses with zinc oxide can pose challenges above 1200 °C. Therefore, apart from possible interactions with zinc oxide, the contribution of iron from the crucible to the slag is limited to the previously described oxygen buffering. In conclusion, iron crucibles will buffer the system to an industrially relevant partial pressure of oxygen, provide the possibility of controlled modification of components, and allow for easy manual handling. The latter aspect allows common muffle, pit, and resistance-heated furnaces to be used, provided that they can be operated in an inert atmosphere.

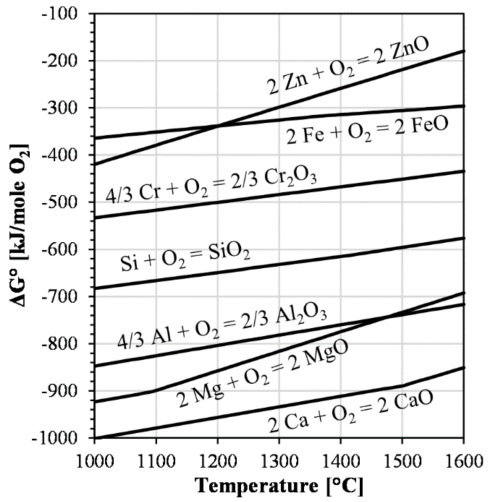

Figure 5. Simplified Ellingham diagram, omitting isolines for the partial pressure of oxygen, calculated using the Reaction module in FactSage 8.2 and the FactPS database [39].

3. Materials and Methods

This chapter includes a general description of the synthesis of iron silicate slags followed by an outline of how the relevance and robustness of this method were evaluated.

3.1. Synthesizing Iron Silicate Slags

The approach to synthesizing iron silicate slags suitable for evaluating inherent reactivity in SCM applications was based on the logic presented in Section 2. Three main characteristics of the synthesis can be identified: using iron crucibles; remelting in an inert atmosphere; and granulating in water jets.

In the present work, the FeO-SiO_2-CaO-Al_2O_3-MgO-Cr_2O_3-system was synthesized, but components can be included or removed if deemed appropriate. The idea of including chromium(III) oxide was based on its characteristics in the industrial process. Chromium, coming from, e.g., refractories and electronic scrap, is a strong nucleation agent in industrial slags [44], leading to the crystallization of chromium-rich spinel phases [45]. Due to the importance of the amorphous content in SCM applications [28,46,47] and the lower activation energy for heterogeneous compared to homogeneous crystallization [48], chromium was considered significant to include for the relevance of the experimental approach.

This methodology includes dry mixing powder chemical reagents in amounts according to the chosen synthetic composition and its total mass. As the current description of this methodology is on a general level, the ratios of the chemicals for a specific composition are omitted. Nonetheless, for the abovementioned slag system, the chosen chemicals were iron (99% Fe), iron(III) oxide (98% Fe_2O_3), silica (99.5% SiO_2), calcium carbonate (99.5% $CaCO_3$), alumina (99.9% Al_2O_3), magnesia (99.95% MgO), and chromium(III) oxide (99.6% Cr_2O_3). The two iron phases were mixed in proportions resulting in iron(II) oxide. The approach of using the two iron compounds, as well as including calcium carbonate rather than calcium oxide, originates from the instabilities of reagent grade iron(II) oxide and calcium oxide in ambient conditions.

After mixing the chemicals, the blend was transferred to an iron crucible (>99.82% Fe) and melted under an inert gas atmosphere in a graphite resistance-heated furnace (Ruhstrat, Göttingen, Germany), Figure 6. The atmosphere was attained by injecting argon (99.999% Ar) and nitrogen (99.996% N_2) at flow rates of 3 L/min and 12 L/min ambient temperature and pressure, respectively. In the experiments, a fixed heating rate of 10 °C/min was used, and the final temperature was based on superheating of 100 °C above the calculated liquidus temperature for the theoretical synthetic slag composition. In the present work, the liquidus temperature was calculated using the Equilib module of FactSage 8.2 with the GTOx database [37–39]. After reaching the final temperature, the slag was homogenized isothermally for 120 min.

Following the homogenization, the crucible was removed manually from the furnace, and the slag was tapped into water jets operating with cold tap water with a flow rate of 1.1 L/s. Information on the granulation equipment used in the present study can be found in a previous publication [19]. Since the crucible was removed directly after the isothermal hold, the experimental layout required careful placement of the thermocouple and the gas injection lances. In the experiments, the time between the removal of the crucible from the furnace to the first contact with the water jets was kept within 15 s. This time necessitates the superheating of the slag to avoid crystallization during handling.

After drying the granulated slag, it can be subjected to analyses relevant to evaluating the success of the synthesis and experiments for assessing properties, such as inherent reactivity.

3.2. Relevance of Methodology

Assessing the relevance of the developed methodology refers to ensuring that granulation in laboratory and industrial scales generates slags with comparable properties. For this purpose, a spot sample of water-granulated iron silicate copper slag, with a true density of 3.44 g/cm^3, was collected from Boliden Rönnskär in Sweden. The sample was taken after

the dewatering process, as illustrated in the flow sheet presented by Isaksson et al. [49]. After drying the slag, representative samples were generated with a Jones riffler, and each analysis or experiment using the industrial slag described in the text below was performed on such a subsample.

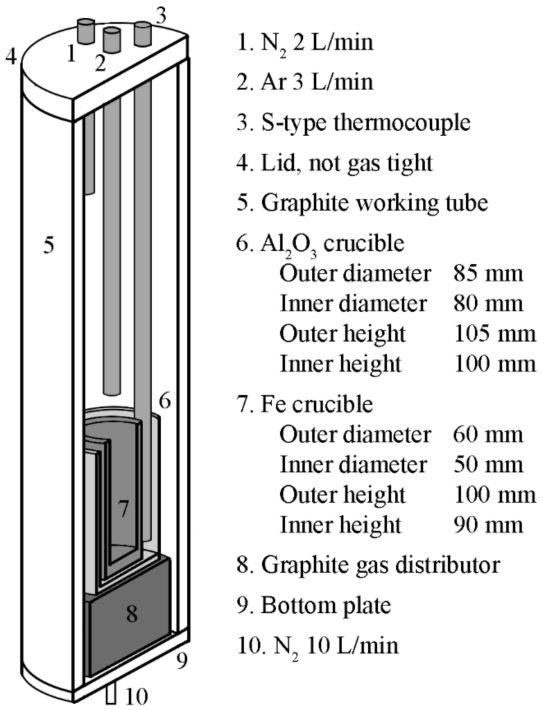

Figure 6. Overview of the experimental setup.

The bath temperature in the settling furnace, from where the industrial slag is tapped and granulated, was unknown for the slag used in the present study. However, reported operational temperatures vary between 1210 and 1288 °C [45,50]. Furthermore, toward the end of tapping the furnace, temperatures exceeding 1300 °C are common due to continued electrical heating [50]. Therefore, three samples were generated in the laboratory scale experiments, each distinguished by their designated homogenization temperature in the laboratory scale furnace, i.e., 1200, 1300, and 1400 °C. As such, the relevance of this methodology was evaluated based on the original slag, granulated on an industrial scale, and the three laboratory-scale samples remelted in iron crucibles and granulated according to the procedure outlined in Section 3.1. The nomenclature used to refer to the samples is presented in Table 2.

Table 2. Sample list for evaluation of relevance.

Label	Granulation	Temperature [°C]
Original slag	Industrial scale	Unknown [1]
1200 °C	Laboratory scale	1200
1300 °C	Laboratory scale	1300
1400 °C	Laboratory scale	1400

[1] Elaborated in the text.

The chemical composition of the original slag was determined by X-ray fluorescence (XRF) spectrometry on a pressed powder sample. For the analysis, a SPECTRO XEPOS energy dispersive XRF spectrometer (SPECTRO, Kleve, Germany) equipped with binary palladium–cobalt anode was used. The instrument was calibrated with in-house standard samples from Boliden Rönnskär.

The four-slag samples were ground individually using 45 mL tungsten carbide grinding bowls in a FRITSCH Pulverisette 7 planetary ball mill (FRITSCH GmbH, Idar-Oberstein,

Germany). Two separate cycles were employed to reach a fine particle size distribution without excessive time spent under grinding. The first cycle was performed at 600 revolutions per minute (RPM) for 3 min using 7 WC balls of 15 mm in diameter. Subsequently, a second cycle of fine grinding was performed using 180 WC balls of 5 mm in diameter for 1 min at 600 RPM. The coarse grinding was based on roughly 12 mL of a representative sample of slag granules, and the fine grinding was, subsequently, performed on the material from the first step.

Rietveld powder X-ray diffraction (XRD) with an internal standard was used to determine the amorphous content of the four slags. Based on possible present phases, calcite (99.5% $CaCO_3$) was determined to be a suitable internal standard to avoid overlapping peaks. In accordance with the published literature [23,31,51], the chosen internal standard was mixed to obtain 10 wt.% in the samples. Mixing was made using a ring mill, and the subsequent scans were performed between 10 and 90 °2θ with copper K_α generated at 45 kV and 40 mA using a Malvern Panalytical Empyrean X-ray diffractometer (Malvern Panalytical, Malvern, UK). The refinement was performed using HighScore+ and the COD database [52].

The iron silicate slags were subjected to the isothermal calorimetry-based rapid screening test for SCMs outlined by Snellings and Scrivener [22], further developed and referred to as the rapid, relevant, and reliable (R^3) test by Avet et al. [53]. The choice of this method was based on the study presented by Li et al. [54], which demonstrated that the R^3 test results correlated strongly with the strength of mortars, independent of the type of SCM and with great repeatability between laboratories. Furthermore, this calorimetry-based testing method tests the inherent reactivity of the SCM without the influence of cement hydration [21,32].

A 3:1 mass-based ratio between portlandite (98% $Ca(OH)_2$) and the ground slags were mixed together with potassium sulfate (99.99% K_2SO_4) on a dry basis. The amount of potassium sulfate was based on the analyzed alumina content of the original slag to achieve a 1:1 SO_3:Al_2O_3 molar ratio. Pastes with 1:1 mass-based ratios of 0.5 M potassium hydroxide solution and the solid blends were mixed for 2 min at 1600 RPM using an overhead stirrer. About 15 g of the pastes was transferred to calorimeter glass ampoules and subsequently placed in a TAM Air isothermal calorimeter (TA Instruments, New Castle, DE, USA). The sealed ampoules were placed in the calorimeter within 5 min after adding the potassium hydroxide solution to the solid blends. The heat flow was recorded for 7 days at a temperature of 40 °C. All weights were recorded on the third decimal point.

Due to the importance of the granulometric properties of SCMs [23–26], the ground slags were characterized for their Brunauer, Emmett, and Teller (BET) specific surface areas. This was achieved by using a Micromeritics Gemini 2390a after degassing at 300 °C for 60 min using a Micromeritics FlowPrep 060 (Micromeritics Instruments Corporation, Norcross, GA, USA).

3.3. Robustness of Methodology

In order to test the robustness of the experimental setup, a triplicate of a synthetic iron silicate slag was synthesized; i.e., three individual samples of the same slag were generated. In accordance with Section 3.1, the chosen system was the FeO-SiO_2-CaO-Al_2O_3-MgO-Cr_2O_3-system, and the aimed composition is presented in Table 3. The concentrations were partially based on the industrial slag of the present study and partially on the literature data, as elaborated in Section 4.1.

Following the procedure outlined in Section 3.1, the chemical reagents for the three slags were mixed individually for each sample. The liquidus temperature was calculated to 1137 °C, which means that the homogenization of the melt was performed at 1237 °C. After water granulation, the slags were dried and labeled A, B, and C.

Table 3. Theoretical composition of synthetic slags.

Component	Concentration [wt.%]
FeO	47.50
SiO_2	39.72
CaO	5.63
Al_2O_3	4.97
MgO	1.99
Cr_2O_3	0.19

Each slag was ground and subjected to XRD analyses with the internal standard, BET-specific surface area measurements, and R^3 isothermal calorimetry, according to the procedures described in Section 3.2. Furthermore, their particle size distributions were determined using laser diffraction by employing a Malvern Mastersizer 3000 (Malvern Panalytical, Malvern, UK). The measurements were performed in an ultrasound-dispersed water suspension, and the results were evaluated using the Fraunhofer approximation. Finally, the chemical composition of each slag was determined by inductively coupled plasma sector field mass spectrometry (ICP-SFMS). The digestion of the samples prior to the ICP-SFMS analyses was achieved via microwave-assisted dissolution in a mixture of hydrochloric acid, nitric acid, and hydrofluoric acid after fusion with lithium metaborate.

4. Results and Discussion

4.1. Relevance of Methodology

The concentrations of the major constituents in the original slag are presented in Table 4. As previously stated, prior to water granulation, the slag undergoes a reduction process to remove zinc. Since the reduction progress to partial pressures of oxygen close to the reduction of ferrous iron to metallic iron, the analysis in Table 4 is presented as ferrous iron rather than ferric. The chemical composition of the sample is within normal variations at the smelter, and, as such, it represents a viable choice for evaluating the relevance of the developed method.

Table 4. Normalized chemical composition of the sample (note roundoff error to 100.1%).

Component	Concentration [wt.%]
FeO	46.2
SiO_2	40.7
CaO	2.9
Al_2O_3	5.2
MgO	1.3
ZnO	1.2
Cu	0.8
Na_2O	0.7
K_2O	0.6
S	0.3
Cr_2O_3	0.2

As evident from the comparison of Tables 3 and 4, the composition of the synthetic slags was intentionally designed to deviate from the industrial slag. The basis for the synthetic triplicate sample was the wider operational window for calcium oxide and alumina, outside the scope of a single smelter, in accordance with the widespread compositions reported in the literature and illustrated in Figure 7. However, the FeO/SiO_2 ratio was placed at the lower end of the spectrum to maintain the relevance for the specific smelter of the present study, which still complies with several previously studied slags. Furthermore, the data highlights, once more, the need for a methodology to generate slags that can be compared on a fair basis. As outlined in Section 1, the origin of the slags in Figure 7 differs in terms of cooling conditions, degree of crystallinity, composition, and grinding.

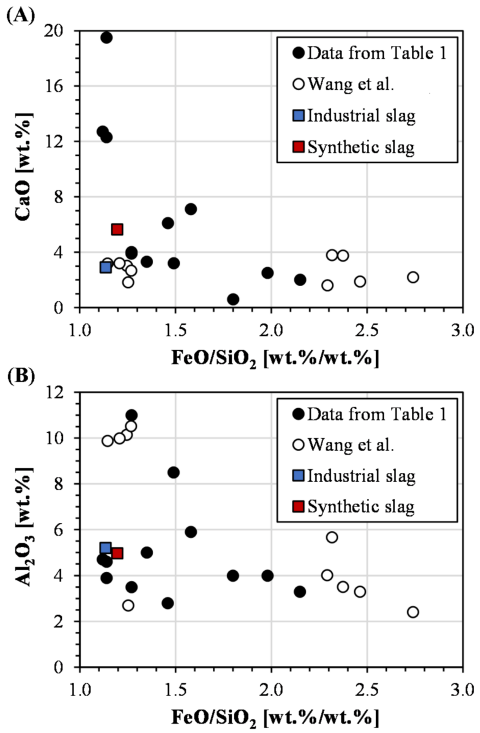

Figure 7. The literature data on previously studied compositions [18] compared to the industrial and synthetic slags of the present study. (**A**) CaO vs. FeO/SiO_2 ratio, and (**B**) Al_2O_3 vs. FeO/SiO_2 ratio.

Studies assessing iron silicate copper slags for SCM applications show substantial crystallization of, e.g., fayalite [10–12,17,18,20], magnetite [10,11,17–20], monticellite (possibly misevaluated kirschsteinite) [17], hedenbergite [18], and calcium sulfate dihydrate [18]. If the aim is to evaluate the effect of chemical composition, the cooling procedure must generate an amorphous slag since only a few crystalline phases show pozzolanic behavior [46]. More specifically, crystalline materials other than, e.g., zeolites and certain minerals in calcareous fly ashes can be considered inert [28,46,47]. Another effect of crystallization is that the overall chemical composition of the slag no longer represents the reactive amorphous phase, which further complicates the intended comparison. The diffractograms of the original slag and the three slags granulated on a laboratory scale are presented in Figure 8. The figure illustrates that the laboratory scale granulation successfully generated an amorphous material for all three temperatures, which shows that laboratory scale granulation is a relevant cooling method for the slag.

Another parameter varying between previously published studies on iron silicate slags is the grinding procedure and, subsequently, the resulting particle size distribution. Ramanathan et al. [24] summarized that the fineness of SCMs has been suggested to be of more importance for reactivity than the SCMs' chemical compositions. Therefore, comparing different chemical compositions requires the absence of crystallization in combination with similar specific surface areas of the materials. Ideally, reaching these granulometric properties should be achieved under similar input energies from grinding, as excessive grinding has been shown to induce non-breakage effects that possibly could relate to improved reactivity [55]. The original slag and the three remelted slags, granulated on a laboratory scale, were ground using the same conditions in the present study. The specific surface areas were determined to be 0.622, 0.670, 0.702, and 0.705 m^2/g for the original slag, 1200, 1300, and 1400 °C samples, respectively. Although the original slag was slightly coarser, the specific surface areas are within the same range. Based on the above, this methodology generated amorphous slags with comparable specific surface areas, which offers excellent prerequisites for comparing their reactivities.

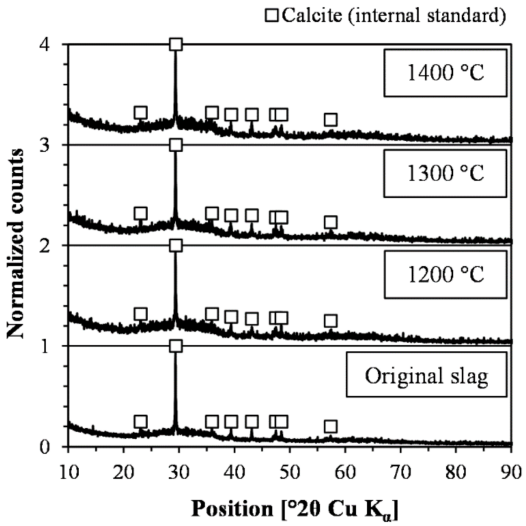

Figure 8. Diffractograms including calcite as internal standard.

Figure 9A illustrates the cumulative heat during 7 days of hydration recorded in the R^3 isothermal calorimeter experiments. An initial high rate of released heat during the first 14 h was recorded, possibly due to a high initial dissolution rate stemming from the entirely amorphous nature of the slags. During the dissolution of the slags, ions are released, which contribute to additional heat generation from the precipitated phase assemblage. Based on previous studies on iron silicate slags [21,32], formed phases could constitute, e.g., calcium silicate hydrate (C-S-H) and calcium aluminum silicate hydrate (C-A-S-H) gels, as well as alumina ferric oxide tri-substituted (AFt) and monosubstituted (AFm). The kink in the cumulative heat, representing a changed heat flow after 14 h, is likely to be related to phase assemblage rather than the dissolution of a specific component since amorphous materials have been shown to dissolve congruently [28]. The progressively lower heat flows, representing the slopes of the curves, result from the gradual consumption of the SCM from dissolution and reactions.

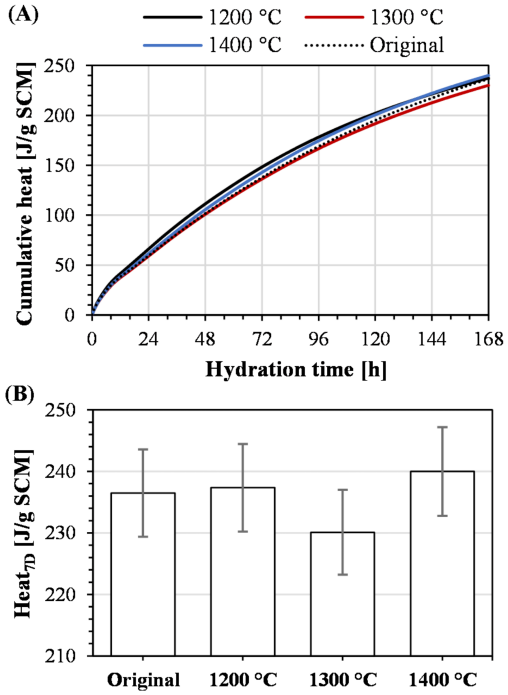

Figure 9. R^3 calorimeter results showing (**A**) cumulative heat and (**B**) evolved heat after 7 days with 3% error bars.

Considering the results presented in Figure 9A, the four slags showed similar heat development patterns. Furthermore, the developed heat after 7 days, presented in Figure 9B, shows that the overall reactivities of the slags are comparable. According to Snellings and Scrivener [22], the R^3 calorimeter experiment has a standard error in the range of 2–3%. Based on these values, error bars of 3% were included in Figure 9B. Accounting for this error in the R^3 experiment, the values presented in Figure 9B do not differ from a statistical standpoint. Therefore, melting iron silicate slags in iron crucibles and granulating in water jets on a laboratory scale generates a slag that has the same reactivity as the industrially granulated slag. Furthermore, this conclusion is valid regardless of homogenization temperature at the achieved cooling rate. Similar observations regarding superheating have been shown for granulated blast furnace slags in a previous publication [56]. Based on the discussion related to the crystallinity of the slags, this conclusion is valid, provided crystallization does not occur due to excessively low homogenization temperatures or inadequate cooling rates.

4.2. Robustness of Methodology

In Section 4.1, the relevance of this methodology was proven, showing that slags granulated on a laboratory scale had similar reactivity as the same slag granulated on an industrial scale. Since the main idea of the present study was to find a method for enabling controlled studies on the effect of changes in chemical composition on reactivity, the repeatability of the synthesis procedure was evaluated. Figure 10 presents the analyzed chemical composition of the triplicate sample. In addition, the theoretical concentrations are included for comparison. The figure illustrates that the concentrations of the major components compare well to the aimed composition. Furthermore, the standard deviation of the population was calculated to be 3.6, 3.6, 2.7, 2.4, and 4.3% of the average value for iron(II) oxide, silica, calcium oxide, alumina, and magnesia, respectively. Therefore, the repeatability of achieving the desired concentrations was considered satisfactory. The minor component, i.e., chromium(III) oxide, was analyzed for 0.12, 0.10, and 0.13 wt.% for samples A, B, and C, respectively, which was less than the aimed concentration of 0.19 wt.%. The low chromium(III) oxide content was considered less important for the subsequent evaluation. More specifically, since the procedure managed to incorporate chromium into the slag, the formation of chromium-rich spinel phases may be facilitated, which satisfies the intended role of chromium in the system.

Based on the diffractograms recorded with internal standards (Figure 11), the three slags were entirely amorphous. Therefore, the intended composition of the slag was successfully incorporated into the amorphous phase, which suggests that synthetic samples suitable for comparing the effect of chemical composition on the reactivity were generated. Furthermore, the chromium content did not facilitate the nucleation and crystallization of phases within the detection limit of the equipment used in the present study. These results are consistent with the results of the industrial slags presented in Section 4.1.

For the industrial slag, grinding generated consistent specific surface areas. However, for samples A, B, and C, the surface areas were measured to be 0.544, 0.418, and 0.474 m^2/g, respectively. Laser diffraction was performed to further assess the differences, and the results (Figure 12) suggested that the grinding successfully produced similar particle size distribution curves. Therefore, based on the specific surface areas, which were consistent with the d_{50} values, the comminution progressed differently between samples. Possibly, the slight variations in chemical composition (Figure 10) could affect the grindability of the slags, especially for increased iron contents. Since the reaction rate depends on the surface area [24], the grinding procedure can be iterated to produce similar granulometric characteristics, which allows for a better comparison of the reactivity in the calorimetry-based testing. However, utilizing a standardized grinding process in the present study was based on the previously reported non-breakage effects introduced by grinding [55].

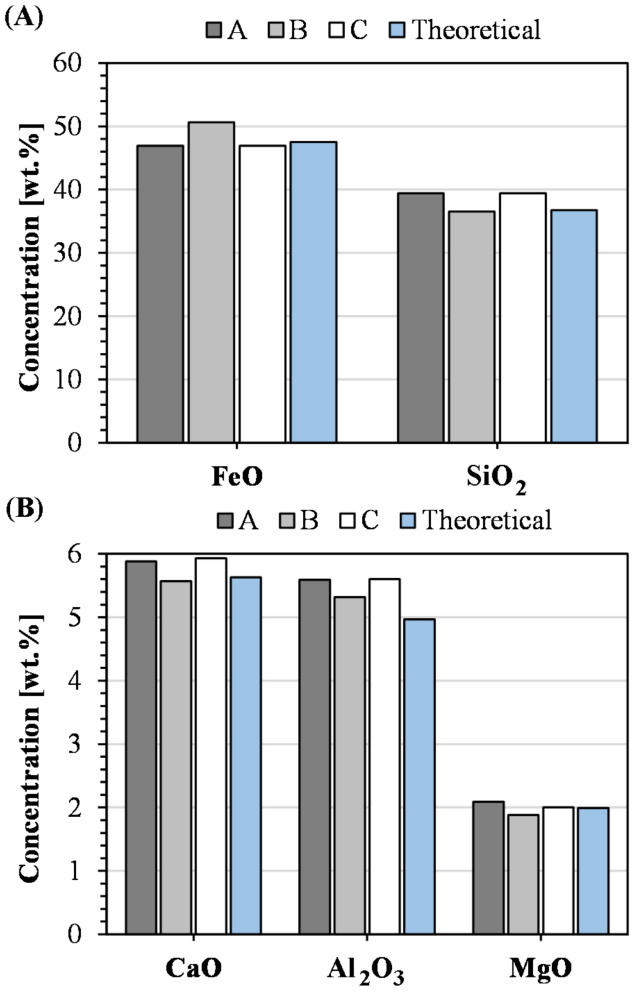

Figure 10. Concentrations of (**A**) FeO and SiO_2, as well as (**B**) CaO, Al_2O_3, and MgO in the synthetic samples compared to the theoretical values.

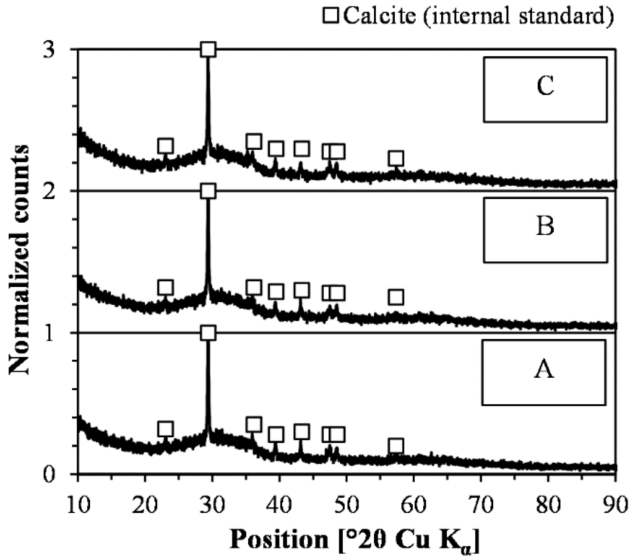

Figure 11. Diffractograms of triplicate samples (denoted A, B, and C) including calcite as internal standard.

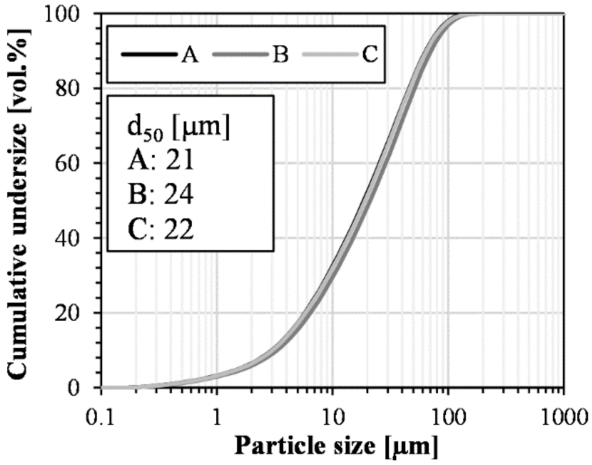

Figure 12. Particle size distributions and d_{50} values for the three samples constituting the triplicate.

Comparing Figures 9A and 13A, the progression of the recorded heat follows a similar pattern, i.e., an initial high reaction rate followed by a kink and, finally, the progressive depletion of the slags from continuous dissolution and reaction. This similarity suggests that the reaction mechanisms of the synthesized slags are not different from the industrial slag. Based on the fact that the synthetic slags successfully integrated the components in an amorphous phase, the observations on the reaction pattern are expected. Furthermore, the developed heat after 7 days, presented in Figure 13B, suggests that the reactivities of the synthetic slags are similar to the industrial slag. Based on the presented chemical composition and specific surface area measurements, there are certain differences between the slags. However, the comparison further suggests that the synthesis generates a relevant sample.

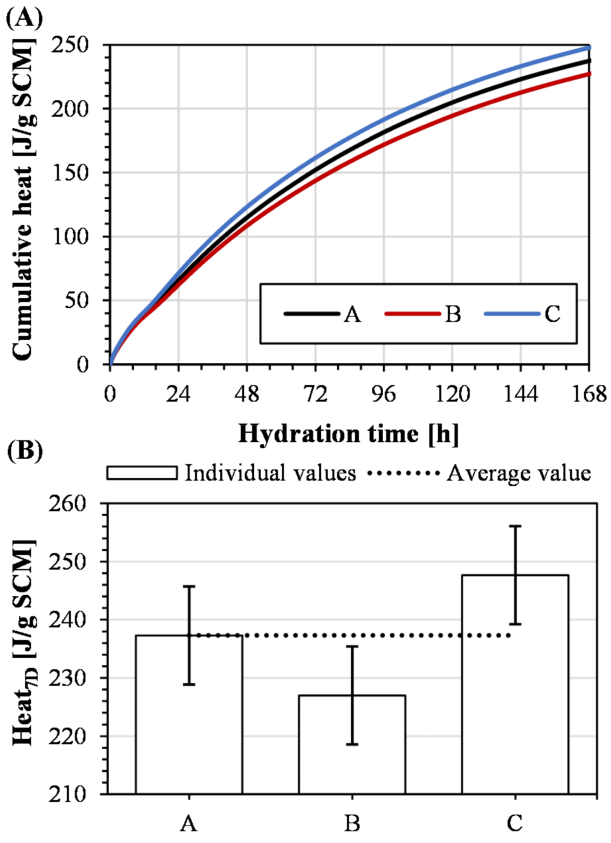

Figure 13. R^3 calorimeter results showing (**A**) cumulative heat and (**B**) evolved heat after 7 days with error bars of one standard deviation.

Figure 13B presents the final values for the developed heat after 7 days, representing the overall reactivity of the slags. The standard deviation based on the population was calculated to be 8.4 J/ g SCM, which corresponds to 3.6% of the average value of the triplicate. Thus, the repeatability of the whole process is considered remarkable since Snellings and Scrivener reported that the standard error of the R^3 isothermal calorimetry test was 2–3% [22]. Comparing Figures 13B and 9B, the repeatability is, however, lower for the synthetic samples in comparison to remelting and granulating an industrial slag. Possibly, this methodology has potential for improvement using iterative grinding aimed at a specific surface area since the differences in reactivity presented in Figure 13B partially follows the variations in specific surface area.

In conclusion, the synthesis of iron silicate slags on a laboratory scale using iron crucibles in an inert atmosphere provides relevant and repeatable results. This offers a methodology to synthesize slags of different compositions, enabling the evaluation of the relationship between chemical composition and inherent reactivity.

5. Conclusions

The present paper introduced a method for synthesizing iron silicate slags suitable for the evaluation of their inherent reactivity in SCM applications. The relevance of this method was verified, concluding the following:

- The reactivity of an industrial slag granulated on an industrial scale does not differ from the reactivity of the same slag granulated using the method developed in the present study;
- Therefore, results on reactivity achieved using this method are directly applicable to industrial slags.

Furthermore, the robustness of this methodology was evaluated by producing a triplicate sample from chemical reagents, concluding the following:

- The targeted chemical composition can be synthesized with high repeatability, and the constituents are successfully incorporated in an entirely amorphous phase;
- The standard deviation of the developed heat in the R3 isothermal calorimeter experiments was 3.6% of the average value of the triplicate, suggesting that this method is robust.

Therefore, the developed method can be used to study the influence of chemical composition on the inherent reactivity of iron silicate slags while generating results that translate directly to industrial slags. Furthermore, the results suggest that iron silicate glasses suitable for SCM applications can be generated outside the context of the copper-making process. The implications suggest that synthesizing iron silicate slags can be used to identify the optimal composition for reactivity as well as study mechanisms that are lost in the noise of uncontrolled parameters when comparing copper slags from different smelters.

Author Contributions: Conceptualization, A.A., L.B., A.L., Å.R. and F.E.; methodology, A.A. and L.B.; formal analysis, A.A. and L.B.; investigation, A.A. and L.B.; writing—original draft preparation, A.A.; writing—review and editing, A.A., L.B., A.L., Å.R. and F.E. All authors have read and agreed to the published version of the manuscript.

Funding: The financial support by Boliden AB was limited to funding, i.e., the participating researchers determined the design of this study, the collection, analysis, and interpretation of data, as well as the writing of the manuscript.

Institutional Review Board Statement: Not applicable.

Informed Consent Statement: Not applicable.

Data Availability Statement: All data is available in this paper.

Acknowledgments: The work was conducted within the Centre of Advanced Mining and Metallurgy (CAMM) at Luleå University of Technology. The assistance of Britt-Louise Holmqvist and Jakob Kero Andertun is greatly acknowledged.

Conflicts of Interest: The authors declare no conflict of interest.

References

1. Gabasiane, T.S.; Danha, G.; Mamvura, T.A.; Mashifana, T.; Dzinomwa, G. Environmental and Socioeconomic Impact of Copper Slag—A Review. *Crystals* **2021**, *11*, 1504. [CrossRef]
2. Shi, C.; Meyer, C.; Behnood, A. Utilization of Copper Slag in Cement and Concrete. *Resour. Conserv. Recycl.* **2008**, *52*, 1115–1120. [CrossRef]
3. International Copper Study Group. *The World Copper Factbook 2022*; International Copper Study Group: Lisbon, Portugal, 2022; p. 11.
4. Kero Andertun, J.; Samuelsson, C.; Peltola, P.; Engström, F. Characterisation and Leaching Behaviour of Granulated Iron Silicate Slag Constituents. *Can. Metall. Q.* **2022**, *61*, 14–23. [CrossRef]
5. Murari, K.; Siddique, R.; Jain, K.K. Use of Waste Copper Slag, a Sustainable Material. *J. Mater. Cycles Waste Manag.* **2015**, *17*, 13–26. [CrossRef]
6. Al-Jabri, K.S.; Taha, R.A.; Al-Hashmi, A.; Al-Harthy, A.S. Effect of Copper Slag and Cement By-Pass Dust Addition on Mechanical Properties of Concrete. *Constr. Build. Mater.* **2006**, *20*, 322–331. [CrossRef]
7. Benhelal, E.; Shamsaei, E.; Rashid, M.I. Challenges against CO_2 Abatement Strategies in Cement Industry: A Review. *J. Environ. Sci.* **2021**, *104*, 84–101. [CrossRef] [PubMed]
8. Olivier, J.G.J.; Janssens-Maenhout, G.; Peters, J.A.H.W. *Trends in Global CO_2 Emissions; 2012 Report*; PBL Netherlands Environmental Assessment Agency: The Hauge, The Netherlands, 2012; pp. 16–17.
9. Lothenbach, B.; Scrivener, K.; Hooton, R.D. Supplementary Cementitious Materials. *Cem. Concr. Res.* **2011**, *41*, 1244–1256. [CrossRef]
10. Tixier, R.; Devaguptapu, R.; Mobasher, B. The Effect of Copper Slag on the Hydration and Mechanical Properties of Cementitious Mixtures. *Cem. Concr. Res.* **1997**, *27*, 1569–1580. [CrossRef]
11. Moura, W.A.; Gonçalves, J.P.; Lima, M.B.L. Copper Slag Waste as a Supplementary Cementing Material to Concrete. *J. Mater. Sci.* **2007**, *42*, 2226–2230. [CrossRef]
12. De Rojas, M.I.S.; Rivera, J.; Frías, M.; Marín, F. Use of Recycled Copper Slag for Blended Cements. *J. Chem. Technol. Biotechnol.* **2008**, *83*, 209–217. [CrossRef]
13. Singh, J.; Singh, J.; Kaur, M. Copper Slag Blended Cement: An Environmental Sustainable Approach for Cement Industry in India. *Curr. World Environ.* **2016**, *11*, 186–193. [CrossRef]
14. Edwin, R.S.; de Schepper, M.; Gruyaert, E.; de Belie, N. Effect of Secondary Copper Slag as Cementitious Material in Ultra-High Performance Mortar. *Constr. Build. Mater.* **2016**, *119*, 31–44. [CrossRef]
15. Sheng, G.; Wang, B.; Wang, S.; Wang, Z. Pozzolanic Reaction of FeO-SiO_2 Slag with Portlandite. *J. Solid. Waste Technol. Manage* **2016**, *42*, 51–57. [CrossRef]
16. Sivakumar, P.P.; Gruyaert, E.; de Belie, N.; Matthys, S. Reactivity of Modified Iron Silicate Slag as Sustainable Alternative Binder. In Proceedings of the Fifth International Conference on Sustainable Construction Materials and Technologies, London, UK, 15–17 July 2019.
17. He, R.; Zhang, S.; Zhang, X.; Zhang, Z.; Zhao, Y.; Ding, H. Copper Slag: The Leaching Behavior of Heavy Metals and Its Applicability as a Supplementary Cementitious Material. *J. Environ. Chem. Eng.* **2021**, *9*, 105132. [CrossRef]
18. Wang, D.; Wang, Q.; Huang, Z. Reuse of Copper Slag as a Supplementary Cementitious Material: Reactivity and Safety. *Resour. Conserv. Recycl.* **2020**, *162*, 105037. [CrossRef]
19. Feng, Y.; Yang, Q.; Chen, Q.; Kero, J.; Andersson, A.; Ahmed, H.; Engström, F.; Samuelsson, C. Characterization and Evaluation of the Pozzolanic Activity of Granulated Copper Slag Modified with CaO. *J. Clean. Prod.* **2019**, *232*, 1112–1120. [CrossRef]
20. Feng, Y.; Kero, J.; Yang, Q.; Chen, Q.; Engström, F.; Samuelsson, C.; Qi, C. Mechanical Activation of Granulated Copper Slag and Its Influence on Hydration Heat and Compressive Strength of Blended Cement. *Materials* **2019**, *12*, 772. [CrossRef]
21. Sivakumar, P.P.; Matthys, S.; de Belie, N.; Gruyaert, E. Reactivity Assessment of Modified Ferro Silicate Slag by R3 Method. *Appl. Sci.* **2021**, *11*, 366. [CrossRef]
22. Snellings, R.; Scrivener, K.L. Rapid Screening Tests for Supplementary Cementitious Materials: Past and Future. *Mater. Struct.* **2016**, *49*, 3265–3279. [CrossRef]
23. Ramanathan, S.; Perumal, P.; Illikainen, M.; Suraneni, P. Mechanically Activated Mine Tailings for Use as Supplementary Cementitious Materials. *RILEM Techn. Lett.* **2021**, *6*, 61–69. [CrossRef]
24. Ramanathan, S.; Tuen, M.; Suraneni, P. Influence of Supplementary Cementitious Material and Filler Fineness on Their Reactivity in Model Systems and Cementitious Pastes. *Mater. Struct.* **2022**, *55*, 1–25. [CrossRef]
25. Zhang, T.S.; Yu, Q.J.; Wei, J.X.; Zhang, P.P. Effect of Size Fraction on Composition and Pozzolanic Activity of High Calcium Fly Ash. *Adv. Cem. Res.* **2011**, *23*, 299–307. [CrossRef]
26. Mirzahosseini, M.; Riding, K.A. Influence of Different Particle Sizes on Reactivity of Finely Ground Glass as Supplementary Cementitious Material (SCM). *Cem. Concr. Compos.* **2015**, *56*, 95–105. [CrossRef]
27. Schöler, A.; Winnefeld, F.; Haha, M.B.; Lothenbach, B. The Effect of Glass Composition on the Reactivity of Synthetic Glasses. *J Am. Ceram. Soc.* **2017**, *100*, 2553–2567. [CrossRef]

28. Snellings, R. Solution-Controlled Dissolution of Supplementary Cementitious Material Glasses at pH 13: The Effect of Solution Composition on Glass Dissolution Rates. *J. Am. Ceram. Soc.* **2013**, *96*, 2467–2475. [CrossRef]
29. Bignozzi, M.C.; Saccani, A.; Barbieri, L.; Lancellotti, I. Glass Waste as Supplementary Cementing Materials: The Effects of Glass Chemical Composition. *Cem. Concr. Compos.* **2015**, *55*, 45–52. [CrossRef]
30. Skibsted, J.; Snellings, R. Reactivity of Supplementary Cementitious Materials (SCMs) in Cement Blends. *Cem. Concr. Res.* **2019**, *124*, 105799. [CrossRef]
31. Astoveza, J.; Trauchessec, R.; Migot-Choux, S.; Soth, R.; Pontikes, Y. Iron-Rich Slag Addition in Ternary Binders of Portland Cement, Aluminate Cement and Calcium Sulfate. *Cem. Concr. Res.* **2022**, *153*, 106689. [CrossRef]
32. Hallet, V.; de Belie, N.; Pontikes, Y. The Impact of Slag Fineness on the Reactivity of Blended Cements with High-Volume Non-Ferrous Metallurgy Slag. *Constr. Build. Mater.* **2020**, *257*, 119400. [CrossRef]
33. Jak, E.; Hayes, P. Phase Equilibria and Thermodynamics of Zinc Fuming Slags. *Can. Metall. Q.* **2002**, *41*, 163–174. [CrossRef]
34. Sukhomlinov, D.; Klemettinen, L.; Avarmaa, K.; O'Brien, H.; Taskinen, P.; Jokilaakso, A. Distribution of Ni, Co, Precious, and Platinum Group Metals in Copper Making Process. *Metall. Mater. Trans. B* **2019**, *50*, 1752–1765. [CrossRef]
35. Nikolic, S.; Hayes, P.C.; Jak, E. Phase Equilibria in Ferrous Calcium Silicate Slags: Part I. Intermediate Oxygen Partial Pressures in the Temperature Range 1200 °C to 1350 °C. *Metall. Mat. Trans. B* **2008**, *39*, 179–188. [CrossRef]
36. Mysen, B.; Richet, P. *Silicate Glasses and Melts*, 2nd ed.; Elsevier: Amsterdam, The Netherlands, 2019; p. 353.
37. Yazhenskikh, E.; Jantzen, T.; Hack, K.; Müller, M. A New Multipurpose Thermodynamic Database for Oxide Systems. *Rasplawy* **2019**, *2*, 116–124. [CrossRef]
38. GTT-Technologies. *GTOx Version 17 Documentation*; GTT-Technologies: Herzogenrath, Germany, 2022.
39. Bale, C.W.; Bélisle, E.; Chartrand, P.; Decterov, S.A.; Eriksson, G.; Gheribi, A.E.; Hack, K.; Jung, I.H.; Kang, Y.B.; Melançon, J.; et al. Reprint of: FactSage Thermochemical Software and Databases, 2010–2016. *Calphad* **2016**, *55*, 1–19. [CrossRef]
40. Tossavainen, M.; Engstrom, F.; Yang, Q.; Menad, N.; Lidstrom Larsson, M.; Bjorkman, B. Characteristics of Steel Slag under Different Cooling Conditions. *Waste Manag.* **2007**, *27*, 1335–1344. [CrossRef]
41. Lee, C.M.; Fruehan, R.J. Phosphorus Equilibrium between Hot Metal and Slag. *Ironmak. Steelmak.* **2005**, *32*, 503–508. [CrossRef]
42. Allibert, M. *Slag Atlas*, 2nd ed.; VDEh Verlag Stahleisen: Düsseldorf, Germany, 1995; pp. 142–143.
43. Anindya, A.; Swinbourne, D.R.; Reuter, M.A.; Matusewicz, R.W. Distribution of Elements between Copper and FeO_x-CaO-SiO_2 Slags during Pyrometallurgical Processing of WEEE: Part 1—Tin. *Min. Process Extr. Metall.* **2013**, *122*, 165–173. [CrossRef]
44. Lennartsson, A.; Engström, F.; Björkman, B.; Samuelsson, C. Understanding the Bottom Buildup in an Electric Copper Smelting Furnace by Thermodynamic Calculations. *Can. Metall. Q.* **2019**, *58*, 89–95. [CrossRef]
45. Isaksson, J.; Vikström, T.; Lennartsson, A.; Samuelsson, C. Influence of Process Parameters on Copper Content in Reduced Iron Silicate Slag in a Settling Furnace. *Metals* **2021**, *11*, 992. [CrossRef]
46. Kucharczyk, S.; Sitarz, M.; Zajac, M.; Deja, J. The Effect of CaO/SiO_2 Molar Ratio of CaO-Al_2O_3-SiO_2 Glasses on Their Structure and Reactivity in Alkali Activated System. *Spectrochim. Acta A Mol. Biomol. Spectrosc.* **2018**, *194*, 163–171. [CrossRef]
47. Glosser, D.; Suraneni, P.; Isgor, O.B.; Weiss, W.J. Using Glass Content to Determine the Reactivity of Fly Ash for Thermodynamic Calculations. *Cem. Concr. Compos* **2021**, *115*, 103849. [CrossRef]
48. Callister, W.D.; Rethwisch, D.G. *Materials Science and Engineering: An Introduction*, 8th ed.; John Wiley & Sons: Hoboken, NJ, USA, 2010; pp. 350–351.
49. Isaksson, J.; Vikström, T.; Lennartsson, A.; Andersson, A.; Samuelsson, C. Settling of Copper Phases in Lime Modified Iron Silicate Slag. *Metals* **2021**, *11*, 1098. [CrossRef]
50. Kero Andertun, J.; Vikström, T.; Peltola, P.; Samuelsson, C.; Engström, F. Characterisation and Leaching Behavior of CaO-Modified Iron-Silicate Slag Produced in Laboratory and Industrial Scales. *Can. Metall. Q.* **2021**, *60*, 294–305. [CrossRef]
51. Moon, G.D.; Oh, S.; Choi, Y.C. Effects of the Physicochemical Properties of Fly Ash on the Compressive Strength of High-Volume Fly Ash Mortar. *Constr. Build. Mater.* **2016**, *124*, 1072–1080. [CrossRef]
52. Grazulis, S.; Chateigner, D.; Downs, R.T.; Yokochi, A.F.T.; Quirós, M.; Lutterotti, L.; Manakova, E.; Butkus, J.; Moeck, P.; le Bail, A. Crystallography Open Database—An Open-Access Collection of Crystal Structures. *J. Appl. Crystallogr.* **2009**, *42*, 726–729. [CrossRef] [PubMed]
53. Avet, F.; Snellings, R.; Diaz, A.A.; Haha, M.B.; Scrivener, K. Development of a New Rapid, Relevant and Reliable (R3) Test Method to Evaluate the Pozzolanic Reactivity of Calcined Kaolinitic Clays. *Cem. Concr. Res.* **2016**, *85*, 1–11. [CrossRef]
54. Li, X.; Snellings, R.; Antoni, M.; Alderete, N.M.; Haha, M.B.; Bishnoi, S.; Cizer, Ö.; Cyr, M.; De Weerdt, K.; Dhandapani, Y.; et al. Reactivity Tests for Supplementary Cementitious Materials: RILEM TC 267-TRM Phase 1. *Mater. Struct.* **2018**, *51*, 1–14. [CrossRef]
55. Romero Sarcos, N.; Hart, D.; Bornhöft, H.; Ehrenberg, A.; Deubener, J. Rejuvenation of Granulated Blast Furnace Slag (GBS) Glass by Ball Milling. *J. Non. Cryst. Solids* **2021**, *556*, 120557. [CrossRef]
56. Ehrenberg, A. Influence of the Granulation Conditions and Performance Potential of Granulated Blastfurnace Slag—Part 2: Chemistry and Physical Properties. *ZKG Int.* **2013**, *3*, 60–67.